Author(s): Venkateswaran, Ramalingam; Balakrishna, Maravanji; Mobin, Shaikh; Tuononen, Heikki

Title: Copper(I) Complexes of Bis(2-(diphenylphosphino)phenyl) Ether: Synthesis, Reactivity, and Theoretical Calculations

Year: 2007

Version:

Please cite the original version:

Venkateswaran, R., Balakrishna, M., Mobin, S., & Tuononen, H. (2007). Copper(I) Complexes of Bis(2-(diphenylphosphino)phenyl) Ether: Synthesis, Reactivity, and Theoretical Calculations. Inorganic Chemistry, 46(16), 6535-6541. https://doi.org/10.1021/ic7005474

Copper(I) Complexes of Bis(2-(diphenylphosphino)phenyl)ether: Synthesis, Reactivity and Theoretical Calculations

Ramalingam Venkateswaran,[†] Maravanji S. Balakrishna,[†]* Shaikh M. Mobin[§] and Heikki M. Tuononen[‡]

[†]*Phosphorus Laboratory, Department of Chemistry,* [§]*National Single Crystal X-ray Diffraction Facility, Indian Institute of Technology Bombay, Mumbai 400 076, India and* [‡]*Department of Chemistry, University of, Jyväskylä, P. O. Box 35, Jyväskylä, FI-40014, Finland*

Abstract

The tricoordinated cationic Cu^{I} complex [Cu(κ^2-*P*,*P'*-DPEphos)(κ^1-*P*-DPEphos)][BF_4] (**1**) containing a dangling phosphorus center was synthesized from the reaction of [Cu($CH_3CN)_4$][BF_4] with DPEphos in 1:2 molar ratio in dichloromethane. When complex **1** is treated with MnO_2, elemental sulfur or selenium, the uncoordinated phosphorus atom undergoes oxidation to form P=E bond resulting in the formation of complexes of the type [Cu(κ^2-*P*,*P'*-DPEphos)(κ^2-*P*,*E*-DPEphos-E)][BF_4] (**2**, E = O; **3**, E = S; **4**, E = Se) containing Cu-E bond. The zigzag polymeric Cu^{I} complex [Cu(κ^2-*P*,*P'*-DPEphos)(μ-4,4'-bpy)]$_n$[BF_4]$_n$ (**5**) was prepared by the reaction of [Cu($CH_3CN)_4$][BF_4] with DPEphos and 4,4'-bipyridine in equimolar ratio. The stereochemical influences of DPEphos on its coordination behavior are examined by DFT calculations.

*Author to whom correspondence should be addressed. E-mail: krishna@chem.iitb.ac.in (M. S. Balakrishna). Fax: +91-22-5172-3480.

Introduction

Mixed ligand Cu^{I} complexes are of interest because of their luminescent properties, which find applications in construction of sensors and organic light emitting diodes (OLED).[1-4] In recent years, there has been several reports on mixed ligand complexes containing both bis(phosphines) and polypyridyls.[5,6] These complexes have been easily synthesized by treating bis(phosphines) with appropriate metal precursors followed by the addition of N-donor ligands. The mixed ligand systems consisting of both bis(phosphines) and partially functionalized or oxidized ligands are less extensive. However, transition metal complexes containing a variety of dangling phosphorus ligands have been extensively studied.[7] Selective oxidation of one of the phosphorus centers in a bis(phosphine) using H_2O_2, MnO_2, S and Se is very difficult since it always leads to the formation of a mixture of products, which complicates the isolation of the desired product. Often, Staudinger reactions of bis(phosphine)s with organic azides afford partially oxidized mono-phosphineimine derivatives in moderate yield.[8-11] Further, it is more challenging to synthesize a mixed ligand complex consisting of a bis(phosphine) and its mono-oxide derivative. In the last decade, there has been several reports on DPEphos ligand because of its potential applications in various organic transformation reactions.[12-14] Recently, we reported the synthesis of several ruthenium(II) complexes of DPEphos and its iminophosphorane derivative.[10,15] The DPEphos ligand showed several interesting coordination modes with Ru^{II} center depending upon the bulkiness of other N, S and P donors. This investigation was aimed at exploring the reactivity of 3d metals such as Cu^{I} towards DPEphos with considerable stereochemical influences which often produce coordinatively unsaturated yet moderately stable 16–electron complexes with

wide catalytic applications. As a part of our research interest,[16] here we describe the reactions of $[Cu(CH_3CN)_4][BF_4]$ with DPEphos which leads to the formation of interesting tricoordinated Cu^I derivatives containing a free P(III) center which can be readily oxidized with chalcogens. The stereochemical influences of DPEphos on its coordination behavior are substantiated by DFT calculations.

Results and Discussion

Treatment of $[Cu(CH_3CN)_4][BF_4]$ with DPEphos in dichloromethane in 1:2 molar ratio affords the mononuclear complex [Cu(κ^2-*P,P'*-DPEphos)(κ^1-*P*-DPEphos)][BF_4] (**1**) in good yield. The mass spectrum of the complex **1** shows the molecular ion peak at *m/z* 1139.21. The $^{31}P\{^1H\}$ NMR spectrum of **1** shows a single resonance at –15.5 ppm indicating all the four phosphorus centers are equivalent. In contrast to this observation, the solid state structure of complex **1** revealed that the Cu^I center is tricoordinated and one of the phosphorus centers is left uncoordinated (Scheme 1). The ^{31}P NMR spectrum suggests the presence of fluxional behavior in the solution state, since the signal broadens at –50 °C. Analogous reaction of $[Cu(CH_3CN)_4][BF_4]$ with 1,2-bis(diphenylphosphino)ethane (dppe) yielded $[Cu(dppe)_2][BF_4]$ in which Cu^I is tetracoordinated with tetrahedral geometry.[17] This difference in the reactivity may be due to the large-bite diphenyl ether backbone and the overall bulkiness of the DPEphos ligand which probably prevents the fourth P(III) center from establishing a Cu–P bond.

Interestingly, the uncoordinated phosphorus center in complex **1** on treatment with MnO_2, S or Se undergoes oxidation to form the corresponding complexes **2** – **4** which are identified from the mass spectra, where the molecular ion peaks appear at *m/z* 1155.34, 1171.04 and 1219.25, respectively. The ^{31}P NMR spectrum of complex **2**

shows three sets of unresolved multiplets in the region 30.2, –12.1 and –15.1 ppm, respectively, for P(=O), two Ps of the chelating ligand and the copper bound phosphorus center of the mono-oxidized DPEphos. The ^{31}P NMR spectra of complexes **3** and **4** are similar to that of complex **2**. The structures of the complexes **2** and **4** are confirmed by X-ray diffraction studies. Interestingly, the addition of excess of oxidizing agents did not cleave any of the Cu–P bonds.

The reaction of $[Cu(CH_3CN)_4][BF_4]$ with DPEphos and 4,4'-bipyridine in equimolar ratio afforded a coordination polymer $[Cu(\kappa^2\text{-}P,P'\text{-DPEphos})(\mu\text{-}4,4'\text{-bpy})]_n[BF_4]_n$ (**5**) as yellow crystalline solid in good yield. The $^{31}P\{^1H\}$ NMR spectrum of complex **5** shows a single peak at –18.7 ppm, which indicates that both the phosphorus atoms are equivalent. The presence of the 4,4'-bipyridine in complex **5** is confirmed by the aromatic proton resonances at 7.65, 8.80 ppm as broad singlets with appropriate intensities in its ^{1}H NMR spectrum. The polymeric structure of complex **5** in the solid state is revealed by the X-ray structural results discussed below and presented in Figure 4.

Molecular Structures

The complexes **1**, **2**, **4** and **5** are recrystallized from CH_2Cl_2/Et_2O solvent mixture. All these complexes are obtained as colorless crystalline solids except the complex **5** which is yellow in color. The Cu^I center in complex **1** adopts a distorted trigonal planar geometry, which is evident from the sum of the three P–Cu–P bond angles of 357.05°. The uncoordinated dangling phosphorus center is oriented towards Cu^I center at a distance of 3.958 Å which is considerably longer than the sum of van der Waals radii of Cu^I and P (3.20 Å)[18] thus indicating the absence of any bonding interactions. The Cu1–

P1, Cu1–P2 and Cu1–P3 bond distances are 2.2686(8), 2.2719(8) and 2.2782(9) Å, respectively, and are comparable with those of [Cu(κ^2-*P*,*P*'-DPEphos)(μ-NN)][BF_4] (2.2614(9), 2.2712(7) Å) (NN = 2,9-dimethyl-1,10-phenanthroline or 2,9-di-*n*-butyl-1,10-phenanthroline).[5]

The geometry around copper in complex **2** is pseudo-tetrahedral. The Cu1–P4, Cu1–P3 and Cu1–P2 bond distances are 2.2855(2), 2.2860(16), 2.2953(15) Å, respectively, which are slightly longer than those in complex **1**. The Cu–O bond distance is 2.356(5) Å, which is slightly longer than those observed in complexes [Cu(dppeO)$_2$][OTf] (2.117(6) Å) and [Cu(BozPHOS)$_2$][OTf] (2.127(19), 2.122(19) Å) (BozPHOS = 1,2-Bis(2,5-dimethylphospholano)benzene mono-oxide).[19,20] In complex **4**, the Cu^I atom exists in distorted tetrahedral geometry. The Cu1–P1 (2.363(1) Å), Cu1–P2 (2.334(1) Å) and Cu1–P3 (2.330(1) Å) bond distances are *ca*. 0.06 – 0.09 Å longer than those found in complex **1**. The P2–Cu1–P3 and P3–Cu1–P1 bond angles of 112.80(3)° and 119.55(3)° are similar to those of complex **2**, whereas the P2–Cu1–P1 bond angle of 108.21(3)° is *ca*. 11.6° less than that in complex **2**. The Cu1–Se1 bond distance of 2.5877(6) Å is comparable with the same (2.675(5), 2.475(4) Å) observed in [Cu(dppfSe)$_2$][BF_4] (dppf = 1,1'-bis(diphenylphosphino)ferrocene).[21]

The X-ray structural determination shows that the complex **5** exists as a zigzag polymer in which copper centers are present in distorted tetrahedral environment. The structure shows couple of non-identical copper centers which are arranged in pairs alternate to each other. The 4,4'-bipyridine acts as the bridging unit between two Cu^I centers to construct a polymeric chain in which the alternate 4,4'-bipyridine rings are distorted with a dihedral angle of 31.42° between the planes of two pyridyl rings,

whereas the adjacent units are coplanar. Generally, the presence of extended conjugation between metal centers and 4,4'-bipyridine units show conducting properties.[22,23] In complex **5**, the extended conjugation is absent due to the twisting of aromatic groups in 4,4'-bipyridine ligands which makes them non-coplanar. This may be due to the packing strain in the solid state which leads to the disorder in the planarity of the 4,4'-bipyridine. The bond angles N2–Cu1–N1, P2–Cu1–P1, N4–Cu2–N3 and P4–Cu2–P3 are 104.46(19)°, 113.28(6)°, 98.81(18)° and 113.71(6)°, respectively.

Theoretical Calculations

To ascertain that the overall bulkiness of the DPEphos ligand is the single factor determining the product of the reaction of $[Cu(CH_3CN)_4][BF_4]$ with DPEphos, DFT calculations were performed for the cationic systems in question. The geometry optimized structure for the three-coordinated $[Cu(\kappa^2\text{-}P,P'\text{-DPEphos})(\kappa^1\text{-}P\text{-DPEphos})]^+$ (see Figure 5a) is in good agreement with the X-ray crystal structure determined for **1**: the calculated values of some key parameters are: Cu1–P1 = 2.326 Å, Cu1–P2 = 2.338 Å, Cu1–P3 = 2.318 Å, ∠P1–Cu1–P2 = 113.8°, ∠P2–Cu1–P3 = 120.7°, ∠P1–Cu1–P3 = 124.3°, and Σ∠PCuP = 358.8°. The average error in the predicted bond lengths is 0.035 Å with single largest deviations observed for Cu–P interactions (*ca.* 0.06 Å longer). The calculated bond angles are also fairly accurate and generally show errors less than 2° for bonds involving C, P, and Cu atoms. On the other hand, the calculated torsional angles show larger deviations from the experimental values. In particular, the torsional angles involving the backbone atoms of the κ^1-*P*-coordinated DPEphos ligand are as much as 10° in error. This results in significantly elongated distance from the uncoordinated phosphorus atom P4 to the Cu^I center in the calculated structure: 4.541 Å (*cf.* 3.958 Å

found in the X-ray crystal structure of **1**). The above discrepancies result mainly from the flat potential energy surface along the Cu1···P4 bond at distances larger than the sum of van der Waals radii for these atoms.

The crystallographic data[24] reported for the cation $[Cu(PPh_3)_4]^+$ was used to build an analogous structure $[Cu(\kappa^2\text{-}P,P'\text{-DPEphos})_2]^+$ in which the Cu^I center is four-coordinated by two DPEphos ligands. The structure of this hypothetical system was optimized with DFT and compared to the structure determined for $[Cu(\kappa^2\text{-}P,P'\text{-DPEphos})(\kappa^1\text{-}P\text{-DPEphos})]^+$ (see Figure 5b). As expected, the coordination of the Cu^I center to four phosphorus atoms instead of three increases the Cu–P bond lengths significantly: the average bond length for the four Cu–P bonds in $[Cu(\kappa^2\text{-}P,P'\text{-DPEphos})_2]^+$ is 2.454 Å. The coordination sphere around the central Cu^I atom in $[Cu(\kappa^2\text{-}P,P'\text{-DPEphos})_2]^+$ is almost ideal tetrahedron as evidenced by the P–Cu–P bond angle range of 104.5 – 111.2°. The bond parameters in the two DPEphos ligands are not significantly different between $[Cu(\kappa^2\text{-}P,P'\text{-DPEphos})_2]^+$ and $[Cu(\kappa^2\text{-}P,P'\text{-DPEphos})(\kappa^1\text{-}P\text{-DPEphos})]^+$ except for the Cu–P–C and C–O–C bond angles, which are opened up by 3 – 6° in the former species due to the increased steric bulk of the two ligands.

To examine the differences and similarities in bonding of $[Cu(\kappa^2\text{-}P,P'\text{-DPEphos})(\kappa^1\text{-}P\text{-DPEphos})]^+$ and $[Cu(\kappa^2\text{-}P,P'\text{-DPEphos})_2]^+$ more closely, the energetics of the process in which two DPEphos ligands chelate a Cu^I center either unsymmetrically or symmetrically were determined. Using the energy decomposition analysis method, the steric and electronic contributions to the chelation energy can be separated as follows:

$$\Delta E_{chelation} = \Delta E_{prep} + \Delta E_{int},$$

in which ΔE_{prep} is the preparation energy required to alter the geometry of two ground states of DPEphos ligands to the geometry they acquire in the overall complex and ΔE_{int} is the interaction energy between the prepared fragments and the Cu^{I} center. The interaction energy ΔE_{int} can further be decomposed into three physically meaningful terms:

$$\Delta E_{int} = \Delta V_{elec} + \Delta E_{Pauli} + \Delta E_{orbital},$$

in which ΔV_{elec} is the classical electrostatic interaction between the unperturbed charge distributions of the prepared fragments, ΔE_{Pauli} is the exchange repulsion component resulting from the destabilizing interactions between the occupied orbitals on each fragment, and the term $\Delta E_{orbital}$ accounts for the stabilizing interactions between the occupied and empty fragment orbitals. The orbital interaction term can additionally be partitioned into contributions from distinct irreducible representations of the interacting system.

As seen from Table 4, the individual P–Cu^{I} interactions are significantly weaker in $[Cu(\kappa^2\text{-}P,P'\text{-DPEphos})_2]^+$ than in $[Cu(\kappa^2\text{-}P,P'\text{-DPEphos})(\kappa^1\text{-}P\text{-DPEphos})]^+$ (170 kJ mol^{-1} per bond *vs.* 250 kJ mol^{-1} per bond), but the total interaction energy term ΔE_{int} is nevertheless more negative for the complex $[Cu(\kappa^2\text{-}P,P'\text{-DPEphos})_2]^+$ which contains one more P–Cu^{I} bond. Hence, if contributions from ΔE_{prep} are neglected, the four-coordinate structure becomes the global energy minimum by approx. 30 kJ mol^{-1}. However, the preparation energy ΔE_{prep} is almost 100 kJ mol^{-1} smaller for the three-coordinate complex than for the four-coordinate cation. This difference in ΔE_{prep} is more than enough to compensate the less favorable bonding interactions in $[Cu(\kappa^2\text{-}P,P'\text{-DPEphos})(\kappa^1\text{-}P\text{-DPEphos})]^+$, which alters the energy of the three-coordinate structure

with a dangling phosphorus center 60 kJ mol^{-1} lower relative to the energy of the symmetric four-coordinate system. Table 4 also shows the contribution of ΔV_{elec}, ΔE_{Pauli}, and $\Delta E_{orbital}$ in ΔE_{int} for both the complexes. We note that the ΔE_{Pauli} term, which is responsible for the steric repulsion, is smaller for $[Cu(\kappa^2\text{-}P,P'\text{-DPEphos})_2]^+$ due to its tetrahedral coordination and, hence, elongated P–Cu^I distances, and that the attractive electrostatic interaction ΔV_{elec} is more negative for $[Cu(\kappa^2\text{-}P,P'\text{-DPEphos})(\kappa^1\text{-}P\text{-DPEphos})]^+$ due to its significantly stronger P–Cu^I interactions (see above). The orbital interaction terms are predicted to be comparable between the two systems.

The above analysis clearly demonstrates that the coordination of a Cu^I center with four phosphorus atoms is, in principle, the energetically most favorable situation, but the entire energy gain will be lost in distorting the two DPEphos ligands to a geometry which facilitates such coordination. Hence, these results confirm that the observed difference in the reactivity of dppe and DPEphos towards $[Cu(CH_3CN)_4][BF_4]$ is in fact due to the overall bulkiness of the DPEphos ligand, which allows *P,P'*-chelation to copper via only one of the two ligands. This was conclusively confirmed by running a full geometry optimization for a three-coordinate structure analogous to $[Cu(\kappa^2\text{-}P,P'\text{-DPEphos})(\kappa^1\text{-}P\text{-DPEphos})]^+$ in which the four phenyl groups in the individual DPEphos ligands were replaced with sterically much less demanding methyl groups. Since the substitution of phenyl to methyl lowers the preparation energy significantly, the interaction energy term now dominates the total chelation energy. Thus, the optimization leads to the immediate coordination of the dangling phosphorus atom to the Cu^I centre, giving a four-coordinate structure with identical Cu–P bonds at 2.345 Å (*cf.* calculated Cu–P bonds in $[Cu(\kappa^2\text{-}$

P,*P'*-DPEphos)$_2$]$^+$ and in [Cu(κ^2-*P*,*P'*-DPEphos)(κ^1-*P*-DPEphos)]$^+$ at 2.454 and 2.326 Å, respectively).

Conclusion

The 16 electron complex [Cu(κ^2-*P*,*P'*-DPEphos)(κ^1-*P*-DPEphos)][BF_4] (**1**) containing one uncoordinated phosphorus center readily undergoes oxidation to form 18 electron complex with Cu-E (E =O, S or Se) bond. The large-bite of diphenyl ether backbone and the overall bulkiness of the ligand play a vital role for this interesting feature of the complex **1**. The complexes **2 - 4** are the first example of mixed-ligand Cu^I bis-chelating complexes containing both bis(phosphine) and its monochalcogenide (PQP=E) derivative. The Cu–O (**2**) and Cu–Se (**4**) bond distances are ca. 0.2 Å longer than those found in analogous compounds. The coordination polymer [Cu(κ^2-*P*,*P'*-DPEphos)(μ-4,4'-bpy)]$_n$[BF_4]$_n$ (**5**) is consists of one dimensional zigzag polymeric structure. The distorted tetrahedral Cu^I centers are connected with 4,4'-bipyridine units and the aromatic rings of alternating units are tilted by an angle of 31.42°. The DFT calculations clearly indicate the stereochemical influences of the ligand framework and the phosphorus substituents on its coordination behavior. We are currently investigating the catalytic utility of tricoordinated Cu^I complex in hydroamination and other related organic transformation reactions.

Experimental

General methods

All manipulations were performed under an atmosphere of dry nitrogen using standard Schlenk techniques. All the solvents were purified by conventional procedure and distilled under nitrogen prior to use.[25] DPEphos[11] and [Cu(CH_3CN)$_4$][BF_4][26] were

prepared according to the published procedures. H_2O_2 (30% solution in water) (Merck), MnO_2 (SD-Fine), sulphur (Merck), selenium (Lancaster) and 4,4'-bipyridine (Aldrich) were purchased from commercial sources and used as received. The ^1H and $^{31}P\{^1H\}$ NMR (δ in ppm) spectra were recorded using Varian 400 Mercury Plus spectrometer operating at the appropriate frequencies using TMS and 85% H_3PO_4 as internal and external references, respectively. Microanalyses were performed on a Carlo Erba Model 1112 elemental analyzer. Electro-spray ionization (EI) mass spectrometry experiments were carried out using Waters Q-Tof micro-YA-105. Melting points were recorded using capillary tubes and are uncorrected.

Syntheses

[Cu(k^2-*P,P′*-DPEphos)(k^1-*P*-DPEphos)][BF_4] (1). A solution of [$Cu(CH_3CN)_4$][BF_4] (0.100 g, 0.318 mmol) in CH_2Cl_2 (8 mL) was added dropwise to a stirring solution of DPEphos (0.342 g, 0.636 mmol) also in CH_2Cl_2 (15 mL) at room temperature. After 8 hours the reaction mixture was concentrated to 5 mL and Et_2O (5 mL) was added and allowed to stay at room temperature for 1 day to obtain colorless crystals of **1**. Yield: 93% (0.363 g, 0.295 mmol). Anal. Calc. for $C_{72}H_{56}O_2P_4CuBF_4$: C, 70.45; H, 4.60%. Found: C, 70.48; H, 4.66%. ^1H NMR (400 MHz, $CDCl_3$) δ 6.44–7.28 (m, *Ph*, 56H). $^{31}P\{^1H\}$ NMR (162 MHz, $CDCl_3$) δ –15.5 (s). MS (EI): *m/z* 1139.21 $[M]^+$.

[Cu(k^2-*P,P′*-DPEphos)(κ^2-*P,O*-DPEphos-O)][BF_4] (2). A mixture of **1** (0.060 g, 0.049 mmol) and MnO_2 (50 mg) in CH_2Cl_2 (5 mL) was stirred for 2 h at room temperature and filtered to obtain a colorless solution, which was concentrated to 3 mL and Et_2O (5 mL) was added to give colorless crystals of **2**. Yield: 87% (0.053 g, 0.042 mmol). Anal. Calc. for $C_{72}H_{56}O_3P_4CuBF_4$: C, 69.55; H, 4.54%. Found: C, 69.19; H, 4.38%. ^1H NMR (400

MHz, $CDCl_3$) δ 6.43–7.45 (m, *Ph*, 56H). $^{31}P\{^1H\}$ NMR (162 MHz, $CDCl_3$) δ 30.2 (q, *P=O*, $^3J_{PP}$ = 6.6 Hz, 1P), –12.1 (s, br, *Cu–P*, 2P), –15.1 (s, br, *Cu–P*, 1P). MS (EI): *m/z* 1155.34 $[M]^+$.

[Cu(κ^2-*P,P'*-DPEphos)(κ^2-*P,S*-DPEphos-S)][BF_4] (3). A mixture of **1** (0.060 g, 0.049 mmol) and elemental sulphur (0.0016 g, 0.049 mmol) in CH_2Cl_2 (5 mL) was stirred for 24 h at room temperature and filtered. The filtrate was concentrated to 3 mL and Et_2O (5 mL) was added to give colorless crystals of **3**. Yield: 76% (0.047 g, 0.037 mmol). Anal. Calc. for $C_{72}H_{56}O_2SP_4CuBF_4$: C, 68.66; H, 4.48; S, 2.55%. Found: C, 68.98; H, 4.62; S, 2.34%. ^1H NMR (400 MHz, $CDCl_3$) δ 5.48–7.60 (m, *Ph*, 56H). $^{31}P\{^1H\}$ NMR (162 MHz, $CDCl_3$) δ 35.5 (t, *P=S*, $^3J_{PP}$ = 26 Hz, 1P), –6.3 (s, br, *Cu–P*, 1P), –9.1 (m, br, *Cu–P*, 1P), –14.1 (m, br, *Cu–P*, 1P). MS (EI): *m/z* 1171.04 $[M]^+$.

[Cu(κ^2-*P,P'*-DPEphos)(κ^2-*P,Se*-DPEphos-Se)][BF_4] (4). Procedure is similar to that of **3**, using selenium (0.004 g, 0.049 mmol). Yield: 82% (0.052 g, 0.040 mmol). Anal. Calc. for $C_{72}H_{56}O_2SeP_4CuBF_4$: C, 66.19; H, 4.32%. Found: C, 66.51; H, 4.58%. ^1H NMR (400 MHz, $CDCl_3$) δ 5.46–8.04 (m, *Ph*, 56H). $^{31}P\{^1H\}$ NMR (162 MHz, $CDCl_3$) δ 22.0 (m, br, *P=Se*, 1P), –7.8 (m, br, *Cu–P*, 2P), –14.2 (s, br, *Cu–P*, 1P). MS (EI): *m/z* 1219.25 $[M]^+$.

[Cu(κ^2-*P,P'*-DPEphos)(μ-4,4'-bpy)]$_n$[BF_4]$_n$ (5). A mixture of $[Cu(CH_3CN)_4]BF_4$ (0.060 g, 0.191 mmol) and DPEphos (0.103 g, 0.191 mmol) in CH_2Cl_2 (10 mL) was stirred for 4 hours at room temperature. 4,4'-bipyridine (0.030 g, 0.191 mmol) in CH_2Cl_2 solution was added to the reaction mixture dropwise and continued stirring for 4 hours to get a clear yellow solution. The reaction mixture was concentrated to 5 mL and Et_2O (5 mL) was added to give yellow crystals of **3**. Yield: 94% (0.152 g). Anal. Calc. for

$C_{46}H_{36}OP_2N_2CuBF_4$: C, 65.38; H, 4.29; N, 3.31%. Found: C, 65.21; H, 4.49; N, 3.21%. ^{1}H NMR (400 MHz, $CDCl_3$) δ 6.71–7.54 (m, *Ph*, 28H), 7.65 (s, *bpy*, 4H), 8.80 (s, br, *bpy*, 4H). $^{31}P\{^1H\}$ NMR (162 MHz, $CDCl_3$) δ –18.7 (s).

Computational Details

DFT calculations were performed primarily for cations $[Cu(\kappa^2\text{-}P,P\text{-DPEphos})_2]^+$ and $[Cu(\kappa^2\text{-}P,P\text{-DPEphos})(\kappa^1\text{-}P\text{-DPEphos})]^+$. The molecular structures were fully optimized by using a combination of the GGA PBEPBE exchange-correlation functional (within the resolution of the identity approximation)[27-30] with the Ahlrichs' triple-zeta valence basis set augmented by one set of polarization functions (def-TZVP). All basis sets were used as they are referenced in the Turbomole 5.9 internal basis set library. Geometry optimizations were performed with Turbomole 5.9.[31] Program ADF 2006.01[32] was used to calculate the individual components of ΔE_{int} in the energy decomposition analysis (EDA). The analysis followed the Morokuma-Ziegler partition scheme[33] and utilized the PBEPBE functional in combination with STO-type all-electron basis sets of TZP quality; scalar relativistic ZORA formalism was also applied in all EDA calculations.

Crystal Structure Determination

Single crystals suitable for X-ray diffraction of **1**, **2**, **4** and **5** were grown by slow diffusion of diethyl ether into dichloromethane solution and mounted on a glass fiber with epoxy resin. Unit cell determination and data were collected on Oxford Diffraction XCALIBUR-S CCD system using Mo Kα radiation (λ = 0.71073Å). The structures were solved and refined by full-matrix least-squares techniques of F^2 using the *SHELX-97* (SHELXL program package).[34] The absorption corrections were done by multi-scan and

all the data were corrected for Lorentz and polarization effects. The non-hydrogen atoms were refined with anisotropic thermal parameters. All the hydrogen atoms were geometrically fixed and allowed to refine using riding model.

Acknowledgements

We are grateful to The Department of Science and Technology (DST) for financial support of this work through grant SR/S1/IC-05/2003. We are thankful to Sophisticated Analytical Instrument Facility (SAIF) IIT Bombay, Department of Chemistry IIT Bombay and National Single Crystal X-ray Diffraction Facility IIT Bombay for instrument facilities. RV is thankful to IIT Bombay for JRF and SRF Fellowships.

Supporting Information Available: X-ray crystallographic files in CIF format for the structure determinations of **1**, **2**, **4** and **5**. This material is available free of charge via the Internet at http://pubs.acs.org.

References

(1) Su, Z.; Che, G.; Li, W.; Su, W.; Li, M.; Chu, B.; Li, B.; Zhang, Z.; Hu, Z. *Appl. Phys. Lett.* **2006**, *88*, 213508.

(2) Armaroli, N.; Accorsi, G.; Holler, M.; Moudam, O.; Nierengarten, J.-F.; Zhou, Z.; Wegh, R. T.; Welter, R. *Adv. Mater.* **2006**, *18*, 1313–1316.

(3) Zhang, Q.; Zhou, Q.; Cheng, Y.; Wang, L.s; Ma, D.; Jing, X.; Wang, F. *Adv. Funct. Mater.* **2006**, *16*, 1203–1208.

(4) Zhang, Q.; Zhou, Q.; Cheng, Y.; Wang, L.; Ma, D.; Jing, X.; Wang, F. *Adv. Mater.* **2004**, *16*, 432–436.

(5) Kuang, S.-M.; Cuttell, D. G.; McMillin, D. R.; Fanwick, P. E.; Walton, R. A. *Inorg. Chem.* **2002**, *41*, 3313–3322.

(6) Cuttell, D. G.; Kuang, S.-M.; Fanwick, P. E.; McMillin, D. R.; Walton, R. A. *J. Am. Chem. Soc.* **2002**, *124*, 6–7.

(7) (a) Balakrishna, M. S.; Ramaswamy, K.; Abhyankar, R. M. *J. Organomet. Chem*. **1998**, *560*, 131–136. (b) Balakrishna, M. S.; Klein, R.; Uhlenbrock, S.; Pinkerton, A. A.; Cavell, R. G. *Inorg. Chem*. **1993**, *32*, 5676–5681. (c) Burrows, A. D.; Mahon, M. F.; Nolan, S. P.; Varrone, M. *Inorg. Chem*. **2003**, *42*, 7227–7238. (d) Wong, E. H.; Prasad, L.; Gabe, E. J.; Bradley, F. C. *J. Organomet. Chem*. **1982**, *236*, 321–331. (e) Bradley, F. C.; Wong, E. H.; Gabe, E. J.; Lee, F. L.; Lepage, Y. *Polyhedron* **1987**, *6*, 1103–1110.

(8) Gololobov, Y. G.; Zhmurova, I. N.; Kasukhin, L. F. *Tetrahedron* **1981**, *37*, 437–472.

(9) Gololobov, Y. G.; Kasukhin, L. F. *Tetrahedron* **1992**, *48*, 1353–1406.

(10) Venkateswaran, R.; Balakrishna, M. S.; Mobin, S. M. *Eur. J. Inorg. Chem* **2007**, 1930–1938.

(11) Balakrishna, M. S.; Santarsiero, B. D.; Cavell, R. G. *Inorg. Chem.* **1994**, *33*, 3079–3084.

(12) Kranenburg, M.; van der Burgt, Y. E. M.; Kamer, P. C. J.; van Leeuwen, P. W. N. M.; Goubitz, K.; Fraanje, J. *Organometallics* **1995**, *14*, 3081–3089.

(13) Kamer, P. C. J.; van Leeuwen, P. W. N. M.; Reek, J. N. H. *Acc. Chem. Res.* **2001**, *34*, 895–904.

(14) van Leeuwen, P. W. N. M.; Kamer, P. C. J.; Reek, J. N. H.; Dierkes, P. *Chem. Rev*. **2000**, *100*, 2741–2769.

(15) Venkateswaran, R.; Mague, J. T.; Balakrishna, M. S. *Inorg. Chem.* **2007**, *46*, 809–817.

(16) (a) Ganesamoorthy, C.; Balakrishna, M. S.; George, P. P.; Mague, J. T. *Inorg. Chem*. **2007**. *46*, 848–858. (b) Punji, B.; Mague, J. T.; Balakrishna, M. S. *Inorg. Chem*. **2006**, *45*, 9454–9464. (c) Punji, B.; Mague, J. T.; Balakrishna, M. S. *J. Organomet. Chem.* **2006**, *691*, 4265–4272. (d) Chandrasekaran, P.; Mague, J. T.; Balakrishna, M. S. *Inorg. Chem*. **2006**, *45*, 6678–6683. (e) Punji, B.; Mague, J. T.; Balakrishna, M. S. *Dalton Trans*. **2006**, 1322-1330.

(17) di Nicola, C.; Pettinari, C.; Ricciutelli, M.; Skelton, B. W.; Somers, N.; White, A. H. *Inorg. Chim. Acta* **2005**, *358*, 4003–4008.

(18) Bondi, A. *J. Phys. Chem.* **1964**, *68*, 441–451.

(19) Saravanabharathi, D.; Nethaji, M.; Samuelson, A. G. *Polyhedron* **2002**, *21*, 2793–2800.

(20) Cote, A.; Charette, A. B. *J. Org. Chem.* **2005**, *70*, 10864–10867.

(21) Pilioni, G.; Longato, B.; Bandoli, G. *lnorg. Chim. Acta* **1998**, *277*, 163–170.

(22) Holliday, B. J.; Swager, T. M. *Chem. Commun.* **2005**, 23–36.

(23) Heeger, A. J. *Angew Chem. Int. Ed.* **2001**, *40*, 2591–2611.

(24) Bowmaker, G. A.; Healy, P. C.; Engelhardt, L. M.; Kildea, J. D.; Skelton, B. W.; White, A. H. *Aust. J. Chem.* **1990**, *43*, 1697–1705.

(25) Armarego, W. L. F.; Perrin, D. D. *Purification of Laboratory Chemicals, 4th ed, Butterworth-Heinemann Linacre House, Jordan Hill, Oxford, U. K.* **1996**.

(26) Kubas, G. J. *Inorg. Synth*. **1979**, *19*, 90.

(27) Perdew, J. P.; Burke, K.; Ernzerhof, M. *Phys. Rev. Lett*. **1996**, *77*, 3865–3868.

(28) Perdew, J. P.; Burke, K.; Ernzerhof, M. *Phys. Rev. Lett*. **1997**, *78*, 1396.

(29) Perdew, J. P.; Ernzerhof, M.; Burke, K. *J. Chem. Phys.* **1996**, *105*, 9982–9985.

(30) Ernzerhof, M.; Scuseria, G. E. *J. Chem. Phys.* **1999**, *110*, 5029–5036.

(31) TURBOMOLE, Program Package for *ab initio* Electronic Structure Calculations, Version 5.9. Ahlrichs, R. *et al.* Theoretical Chemistry Group, University of Karlsruhe, Karlsruhe, Germany, 2006.

(32) ADF2006.01, SCM, Theoretical Chemistry, Vrije Universiteit, Amsterdam, Netherlands, http://www.scm.com.

(33) (a) Ziegler, T.; Rauk, A. Theor. Chem. Acta **1977**, *46*, 1. (b) Ziegler, T.; Rauk, A. Inorg. Chem. **1979**, *18*, 1558. (c) Ziegler, T.; Rauk, A. Inorg. Chem. **1979**, *18*, 1755. (d) Bickelhaupt, F. M.; Baerends, E. J. *Reviews in Computational Chemistry*; Eds. Lipkowitz, K. B.; Boyd, D. B.; Wiley: New York, **2000**, *15*, 1–86.

(34) Sheldrick, G. M. *SHELXS97* and *SHELXL97*; University of Gottingen: Gottingen, Germany, 1997.

Graphics and Tables

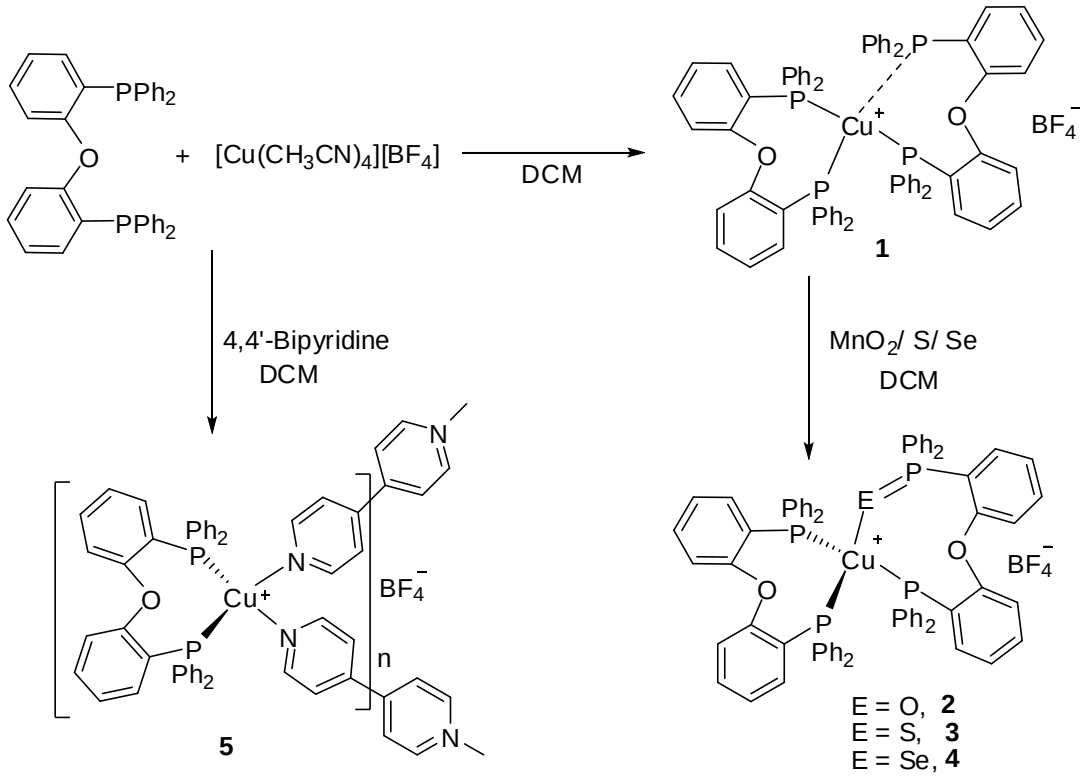

Scheme 1. Synthesis of [Cu(κ^2-*P*,*P*-DPEphos)(κ^1-*P*-DPEphos)][BF_4] (**1**) and [Cu(κ^2-*P*,*P*-DPEphos)(μ-4,4'-bpy)]$_n$[BF_4]$_n$ (**5**). Reactions of **1** with MnO_2, S, Se.

Figure captions

Figure 1. Molecular structure of complex **1**. Hydrogen atoms have been omitted for clarity.

Figure 2. Molecular structure of complex **2**. Hydrogen atoms have been omitted for clarity.

Figure 3. Molecular structure of complex **4**. Hydrogen atoms and uncoordinated solvent molecules have been omitted for clarity.

Figure 4. Molecular structure of complex **5**. Hydrogen atoms and uncoordinated solvent molecules have been omitted for clarity.

Figure 5. Optimized structure of a) [Cu(κ^2-*P*,*P*'-DPEphos)(κ^1-*P*-DPEphos)]$^+$ and b) [Cu(κ^2-*P*,*P*'-DPEphos)$_2$]$^+$.

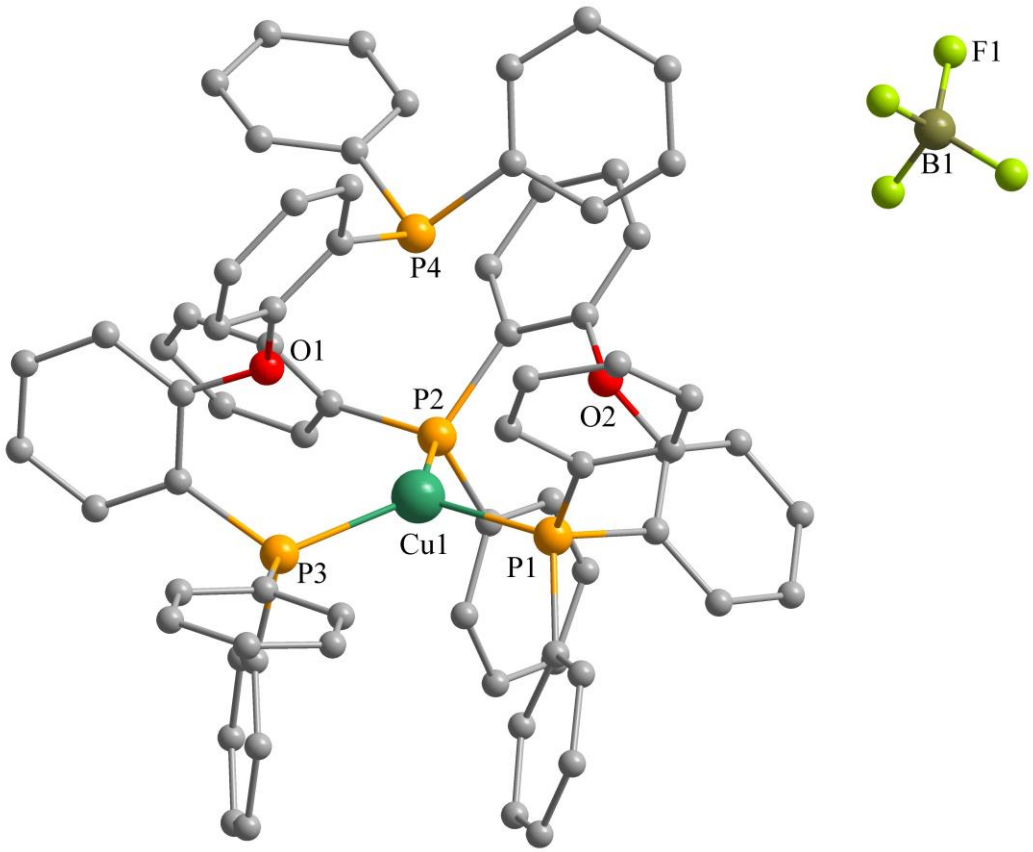

Figure 1

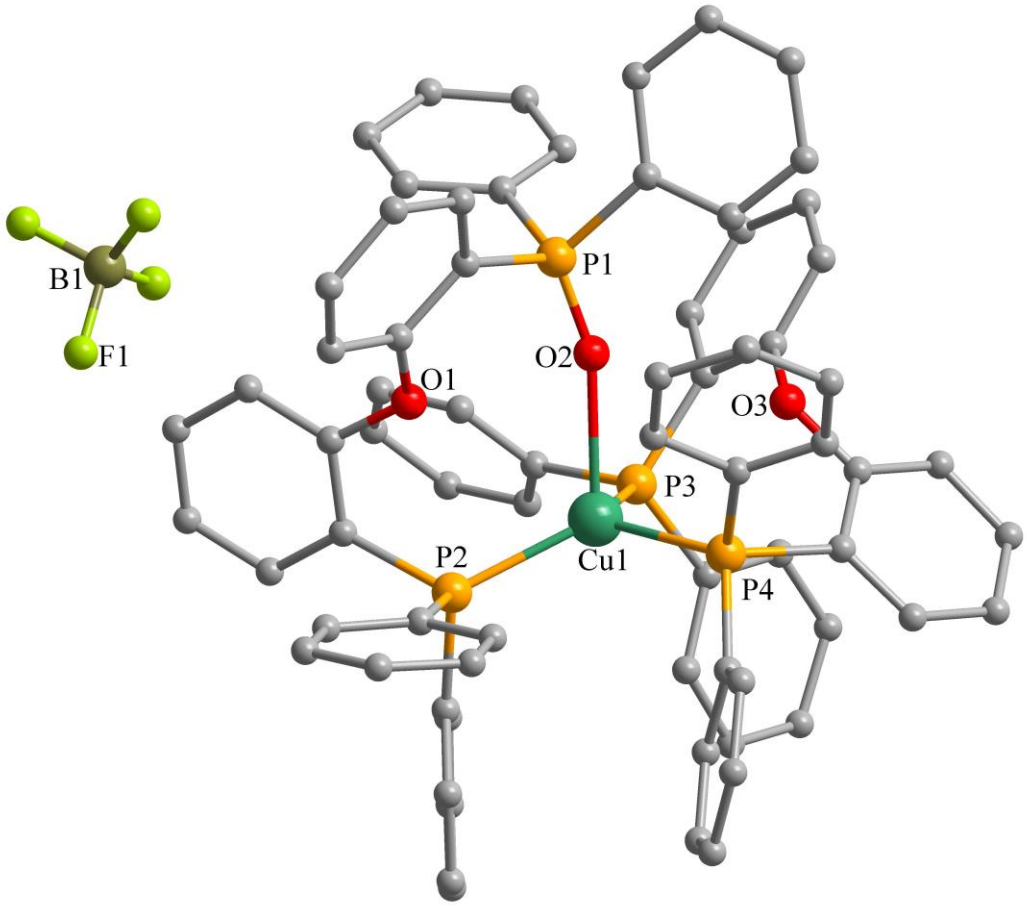

Figure 2

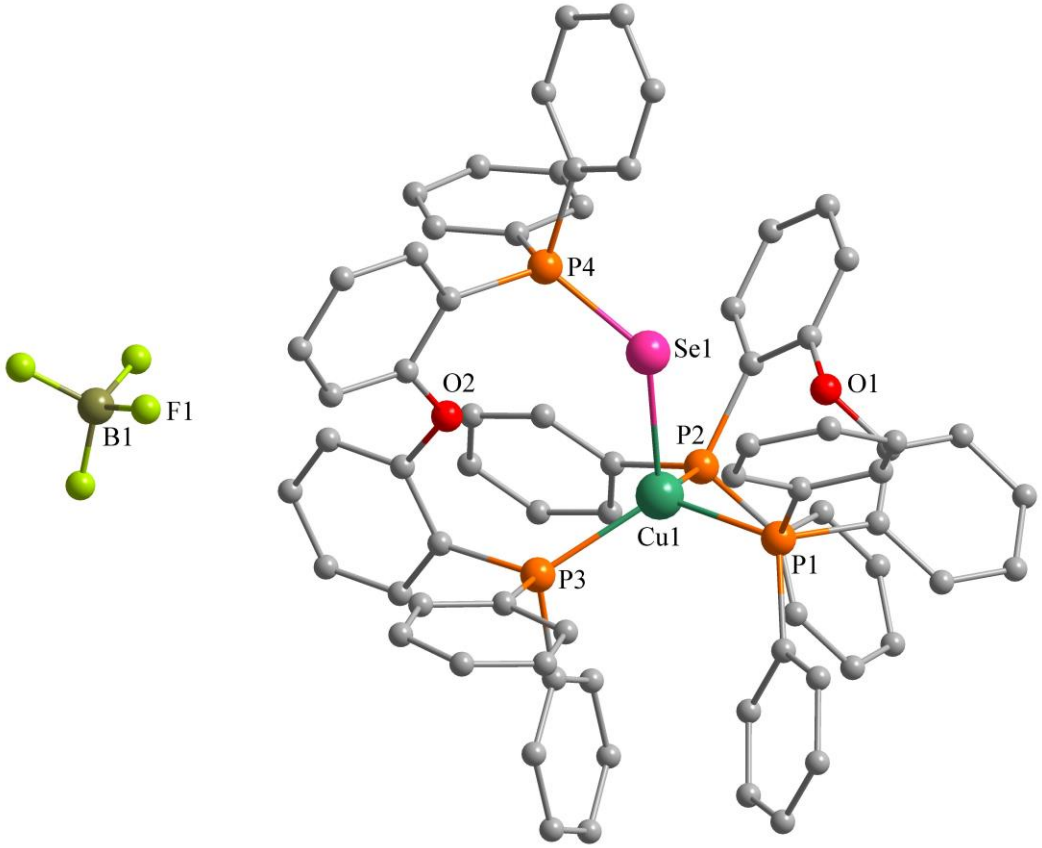

Figure 3

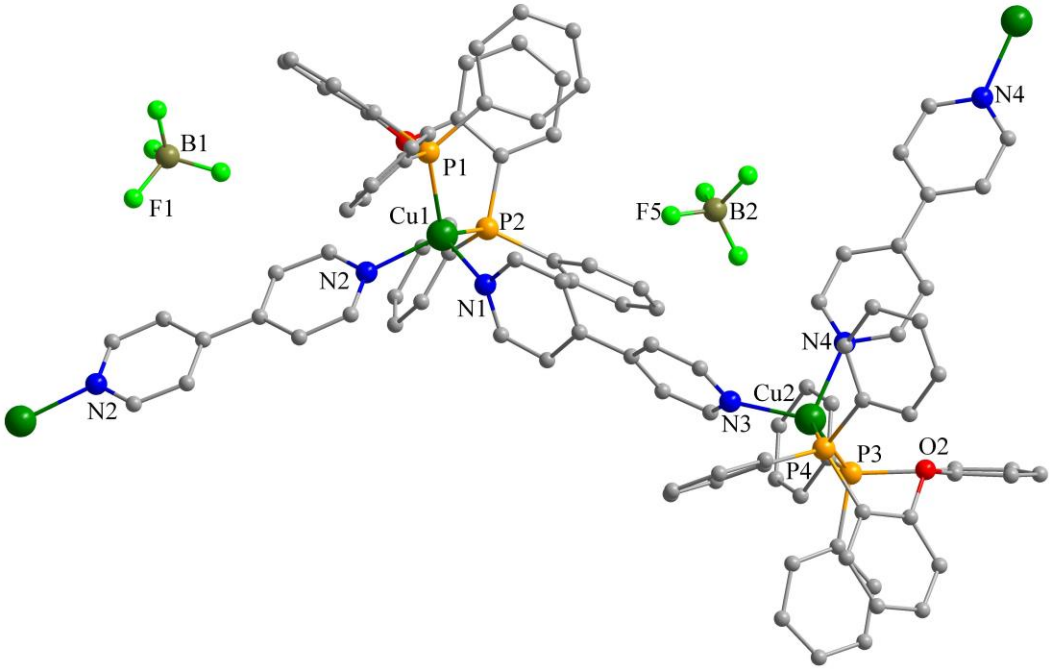

Figure 4

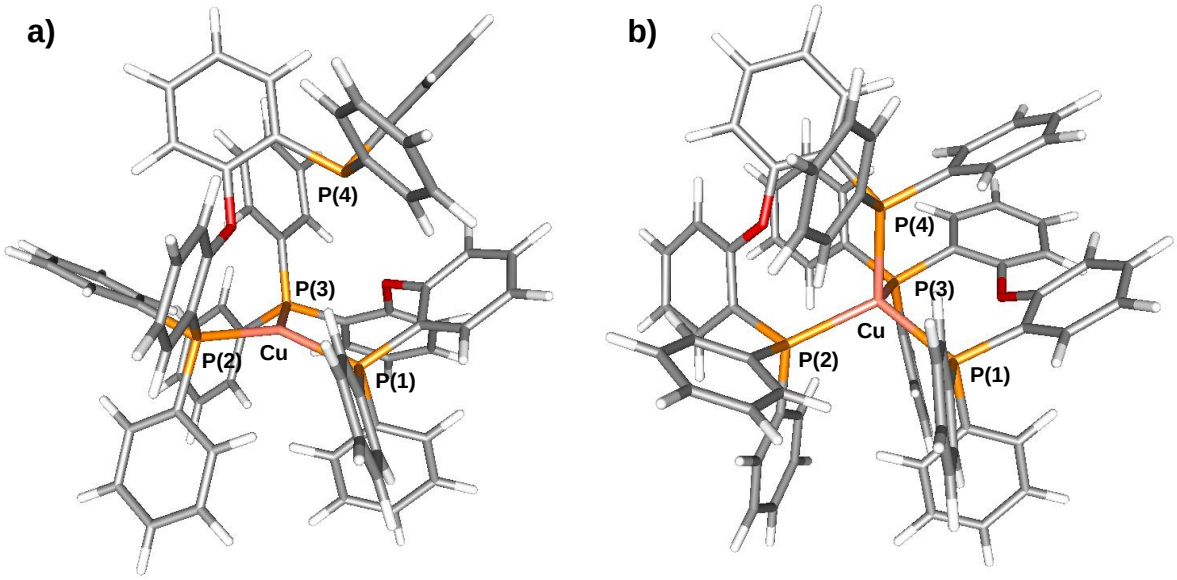

Figure 5

Table 1. Selected bond distances and bond angles for complexes **1** and **2**

Complex **1**				Complex **2**			
Bond distances (Å)		Bond angles (°)		Bond distances (Å)		Bond angles (°)	
Cu1-P1	2.2686(8)	P1-Cu1-P3	121.85(3)	Cu1-P4	2.2855(15)	P4-Cu1-P3	112.52(6)
Cu1-P2	2.2719(8)	P1-Cu1-P2	113.87(3)	Cu1-P3	2.2860(16)	P4-Cu1-P2	119.20(6)
Cu1-P3	2.2782(9)	P3-Cu1-P2	121.33(3)	Cu1-P2	2.2953(15)	P3-Cu1-P2	119.85(6)
B1-F1	1.366(4)	C54-O1-C55	120.5(2)	Cu1-O2	2.356(5)	P4-Cu1-O2	96.41(12)
B1-F2	1.336(4)	C18-O2-C19	117.9(2)	P1-O2	1.463(5)	P3-Cu1-O2	89.39(13)
Cu1···P4	3.958			B1-F1	1.317(7)	P2-Cu1-O2	112.20(12)
				B1-F2	1.318(6)	P1-O2-Cu1	161.6(3)

Table 2. Selected bond distances and bond angles for complexes **4** and **5**

Complex **4**				Complex **5**			
Bond distances (Å)		Bond angles (°)		Bond distances (Å)		Bond angles (°)	
Cu1-P3	2.3303(10)	P2-Cu1-P3	112.80(3)	Cu1-N2	2.072(5)	N2-Cu1-N1	104.46(19)
Cu1-P2	2.3344(9)	P3-Cu1-P1	119.55(3)	Cu1-N1	2.109(5)	N2-Cu1-P2	112.62(15)
Cu1-P1	2.3634(9)	P2-Cu1-P1	108.21(3)	Cu1-P2	2.2762(18)	N1-Cu1-P2	111.34(13)
Cu1-Se1	2.5877(6)	P3-Cu1-Se1	113.60(3)	Cu1-P1	2.2983(17)	N2-Cu1-P1	107.23(14)
P4-Se1	2.1513(9)	P2-Cu1-Se1	106.35(3)	Cu2-N4	2.078(4)	N1-Cu1-P1	107.37(14)
B1-F1	1.373(6)	P1-Cu1-Se1	94.28(3)	Cu2-N3	2.081(5)	P2-Cu1-P1	113.28(6)
B1-F2	1.387(6)	P4-Se1-Cu1	126.09(3)	Cu2-P4	2.2552(17)	N4-Cu2-N3	98.81(18)
				Cu2-P3	2.2846(17)	N4-Cu2-P4	112.13(14)
				B1-F1	1.400(12)	N3-Cu2-P4	116.49(14)
				B1-F2	1.385(12)	N4-Cu2-P3	103.67(14)
						N3-Cu2-P3	110.34(14)
						P4-Cu2-P3	113.71(6)

Table 3. Crystallographic information for complexes **1**, **2**, **4** and **5**

	1	**2**	**4**	**5**
Formula	$C_{72}H_{56}CuO_2P_4BF_4$	$C_{72}H_{56}CuO_3P_4BF_4$	$C_{73}H_{58}BCl_2CuF_4O_{2.5}P_4Se$	$C_{97}H_{78}B_2Cl_{7.5}Cu_2F_8N_4O_2P_4$
fw	1227.41	1243.41	1399.28	2022.09
crystal system	Orthorhombic	Orthorhombic	Triclinic	Triclinic
space group	Pbcn	Pbcn	P -1	P-1
a, (Å)	20.1286(16)	20.187(5)	12.898(2)	13.803(2)
b, (Å)	24.5174(17)	24.542(5)	13.6337(6)	19.089(4)
c, (Å)	24.833(3)	24.756(4)	19.150(2)	20.051(5)
α, (deg)	90	90	104.166(6)	69.255(19)
β, (deg)	90	90	94.444(12)	77.065(16)
γ, (deg)	90	90	94.259(7)	72.710(15)
V, ($Å^3$)	12255(2)	12265(4)	3240.0(7)	4675.5(15)
Z	8	8	2	2
$\rho_{calc,}$ g cm^{-3}	1.331	1.347	1.434	1.436
μ (MoKa), (mm^{-1})	0.520	0.521	1.139	0.805
F (000)	5072	5136	1428	2063
crystal size (mm)	0.22 × 0.26 × 0.33	0.21 × 0.31 × 0.33	0.35 × 0.30 × 0.28	0.17 × 0.21 × 0.33
T (K)	150	293	150	150
2θ range, deg	3.0 – 25.0	3.1 – 25.0	3.0 – 25.0	3.0 – 25.0
Total no. reflns	10745	10546	11256	16433

No. of indep reflns	758 [R_{int} = 0.041]	767 [R_{int} = 0.141]	802 [R_{int} = 0.034]	1141 [R_{int} = 0.072]
GOF (F^2)	1.089	0.776	1.104	1.030
R_1[a]	0.0489	0.0580	0.0388	0.0736
wR_2[b]	0.1502	0.1508	0.1197	0.2066

[a] $R = \Sigma||F_o|-|F_c||/\Sigma|F_o|$.

[b] $R_w = \{[\Sigma w(F_o^2-F_c^2)/\Sigma w(F_o^2)^2]\}^{1/2}$ $w = 1/[\sigma^2(F_o^2)+(xP)^2]$ where $P = (F_o^2+2F_c^2)/3$

Table 4. Energy Decomposition Analysis of [Cu(κ^2-*P*,*P'*-DPEphos)(κ^1-*P*-DPEphos)]$^+$ and [Cu(κ^2-*P*,*P'*-DPEphos)$_2$]$^+$ [a]

	$\Delta E_{chelation}$	ΔE_{prep}	ΔE_{int}	ΔV_{elec}	ΔE_{Pauli}	$\Delta E_{orbital}$
[Cu(κ^2-*P*,*P*-DPEphos)(κ^1-*P*-DPEphos)]$^+$	–740	19	–759	–765	635	–600
[Cu(κ^2-*P*,*P*-DPEphos)$_2$]$^+$	–677	116	–793	–677	528	–610

[a] Energies are reported in kJ mol^{-1}.